Available online at www.sciencedirect.com
ScienceDirect
Journal of Power Sources 162 (2006) 780–789
JOURNAL OF POWER SOURCES
www.elsevier.com/locate/jpowsour

Studies of cycling behavior, ageing, and interfacial reactions of $LiNi_{0.5}Mn_{1.5}O_4$ and carbon electrodes for lithium-ion 5-V cells

Doron Aurbach [a], Boris Markovsky [a,*], Yosef Talyossef [a], Gregory Salitra [a], Hyeong-Jin Kim [b], Seungdon Choi [b]

[a] *Department of Chemistry, Bar-Ilan University, Ramat-Gan 52900, Israel*
[b] *Battery Research and Development, LG Chem. Research Park, Daejeon 305-380, South Korea*

Received 8 February 2005
Available online 18 August 2005

Abstract

The cycling and storage behavior of $LiNi_{0.5}Mn_{1.5}O_4$ and MCMB electrodes for 5-V Li-ion batteries was investigated at elevated temperatures using a variety of electrochemical (CV, EIS) and spectroscopic (XPS, micro-Raman) tools. It was established that $LiNi_{0.5}Mn_{1.5}O_4$ electrodes could be cycled highly reversibly, demonstrating sufficient capacity retention at 60 °C by a constant current/constant voltage mode in DMC–EC/1.5 M $LiPF_6$ solutions. By studying the influence of temperature on the impedance of $LiNi_{0.5}Mn_{1.5}O_4$ electrodes, we conclude that when the initial electrode's surface chemistry is developed at a high temperature (60 °C) it becomes nearly invariant, and hence, their impedance remains steady upon cycling and storage. Prolonged storage of these electrodes at 60 °C may result in local Mn and Ni dissolution and transformation of the active material to λ-MnO_2. We have found that the surface chemistry of aged $LiNi_{0.5}Mn_{1.5}O_4$ electrodes (free of carbon black and PVdF) involves the formation of LiF, C–F and P–F_x species. Storage of MCMB electrodes in $LiPF_6$ containing solutions at open circuit conditions (before their first lithiation) leads to significant morphological changes and the formation of lithium fluoride on the electrode surface, as determined by the XRD studies. LiF is probably a product of a catalytic thermal decomposition of $LiPF_6$. These initial changes further influence the impedance and kinetics of the lithiated electrodes.

Keywords: $LiNi_{0.5}Mn_{1.5}O_4$ electrodes; MCMB electrodes; Cycling behavior; Storage; Impedance; Temperature dependences

1. Introduction

A new class of 5-V Li-ion batteries can become a reality in the near future due to intensive studies by many worldwide research groups of positive electrodes (cathodes) and suitable electrolyte solutions, which operate at high voltages. Possible candidates of electrodes for these batteries are cathodes based on substituted $LiMn_2O_4$-spinel materials of the general formulae of $LiM_xMn_{2-x}O_4$, where manganese is partially replaced by other transition metals: M = Ni, Co, Cu, Cr [1–10], and negative electrodes (anodes) such as mesocarbon microbeads (MCMB) [11–13]. $LiNi_{0.5}Mn_{1.5}O_4$ has some advantages over $LiMn_2O_4$ spinel in a reversible behavior up to 5 V, e.g., sufficient capacity retention, electrochemical stability during prolonged cycling and storage at elevated temperatures in conventional DMC–EC/$LiPF_6$ solutions [14].

This paper is aimed at a further study of the electrochemical performance, storage behavior and possible interfacial reactions of $LiNi_{0.5}Mn_{1.5}O_4$ and MCMB electrodes in a wide range of temperatures in the above solution, operating at potentials up to 5 V.

In this research, we followed the strategy described in a previous paper [15], i.e., the use of as many sources of information as possible in a single study, in order to understand the electrochemical behavior of these systems.

* Corresponding author. Tel.: +972 3 531 8832; fax: +972 3 535 1250.
E-mail address: markovb@mail.biu.ac.il (B. Markovsky).

0378-7753/$ – see front matter © 2005 Elsevier B.V. All rights reserved.
doi:10.1016/j.jpowsour.2005.07.009

2. Experimental

Composite $LiNi_{0.5}Mn_{1.5}O_4$ electrodes on aluminum foil current collectors (one-side loading) were obtained from LG Chem. They comprised the active material (90%), conductive carbon and a PVdF binder. The particle size distribution of the $LiNi_{0.5}Mn_{1.5}O_4$ powder measured by a Mastersizer 2000 (Malvern, UK) was as follows: D 0.1–7.06, D 0.5–14.61, D 0.9–35.11 μm. Composite carbon electrodes (LG Chem.) on copper current collectors comprised MCMB1028 (beads of 10 μm average size), nanoparticles of super P carbon (for better electrical contact among the MCMB particles), and a PVdF binder. For electrochemical measurements, we used two- and three-electrode cells in a coin-type 2325 configuration (NRC, Canada) using a polypropylene separator (Celgard). A lithium disk and a lithium chip served as counter and reference electrodes. The geometric surface area of $LiNi_{0.5}Mn_{1.5}O_4$ or MCMB electrodes exposed to the electrolyte solution was 1.54 cm^2. Three-electrode flooded cells, including $LiNi_{0.5}Mn_{1.5}O_4$ cathodes, lithium foil counter electrodes in parallel plate configuration, and lithium wire reference electrodes were also used. The electrochemical cells were assembled in a glove-box filled with pure argon (VAC, Inc.). The electrolyte solution (Li-battery grade, Tomiyama Pure Chemical Industries, Ltd.) was a mixture of dimethyl carbonate (DMC), ethylene carbonate (EC), 2:1 (w/w) and 1.5 M $LiPF_6$. The concentration of HF in solutions was about 100 ppm and could also contain 20 ppm of water. The electrochemical measurements were carried out using a battery test unit model 1470 coupled with a FRA model 1255 (Solartron, Inc.), and a multichannel battery tester from Maccor, Inc., model 2000. All the potentials are given versus Li/Li^+. The impedance of $LiNi_{0.5}Mn_{1.5}O_4$ electrodes was measured in the 100 kHz to 5 mHz frequency range at equilibrium pre-determined potentials (OCV conditions). The alternating voltage amplitude was 3 mV. All the measurements were conducted in thermostats at 30–60 °C. Impedance spectra were recorded after every five galvanostatic cycles (C/5 rate) at a fully intercalated state (E = 3.50 V), at a partially deintercalated state (E = 4.70 V), and after storage of $Li/LiNi_{0.5}Mn_{1.5}O_4$ cells at the above states. SEM measurements were carried out using a JEOL model JSM-840 scanning electron microscope. Raman spectra of $LiNi_{0.5}Mn_{1.5}O_4$ and MCMB electrodes were collected ex situ, in a back-scattered configuration using a micro-Raman spectrometer HR800 (Jobin Yvon Horiba), holographic grating 1800 grooves mm^{-1}, with an Ar-laser (excitation line 514.5 nm), objective 50× (numerical aperture 0.75). The spectra were obtained from at least three different locations on the electrodes' surfaces. XPS data were obtained with an HX Axis system (Kratos, Inc.), using monochromic Al Kα (1486.6 eV) X-ray beam. For a series of XPS and Raman spectroscopy measurements, some electrodes were prepared by pressing (15,000 psi) of the $LiNi_{0.5}Mn_{1.5}O_4$ powder (ca. 8 mg cm^{-2}) onto both sides of an aluminum foil. By this mode of preparation, the particles of the active material were embedded on the current collector, and thus the electrodes did not contain any binder and carbon black conductive additive. This eliminates possible side effects and allows the recording of the response of the active material only. Storage tests of $LiNi_{0.5}Mn_{1.5}O_4$ and MCMB electrodes were carried out at room temperature (in a glove-box) and at elevated temperatures (in thermostats). Materials (electrodes or powders) used in this study were soaked in solutions in tightly sealed polyethylene vials (assembled under pure Ar atmosphere in a glove-box). Electrolyte solutions, collected after cycling and storage experiments, were analyzed for manganese and nickel content by the ICP technique (ICP-AES, model "Spectroflame Modula E" from Spectro, Kleve, Germany).

3. Results and discussion

3.1. $LiNi_{0.5}Mn_{1.5}O_4$ electrodes

As was shown in our previous work [14], $LiNi_{0.5}Mn_{1.5}O_4$ electrodes demonstrated quite stable and reversible cycling behavior (3.5–4.9 V) in conventional electrolyte solutions at elevated temperatures. We have also shown (SSCV experiments) that electrodes cycled at 60 °C in a DMC–EC (2:1)/1.5 M $LiPF_6$ solution provided high charge/discharge capacities with Coulombic efficiency around 98% [16]. Even after prolonged storage during 30–50 days in a charged state at 60 °C, the electrodes demonstrated reasonable capacity retention (discharge capacity loss was around 0.3% per day). Discharge capacity loss measured from these electrodes during cycling by constant current/constant voltage mode (C/5 rate and then potentiostatic step at E = 4.9 V for 5 h) was calculated as 0.06 mAh g^{-1} per cycle (Fig. 1). In this figure, we compare a typical cycling performance of $LiNi_{0.5}Mn_{1.5}O_4$ electrodes at 25 and 60 °C, and chronopotentiograms recorded during galvanostatic cycles (C/5 rate) at various temperatures. In the potential range of 4.7–4.8 V, these voltage profiles exhibit two plateaus I and II corresponding to Ni^{2+}/Ni^{3+} and Ni^{3+}/Ni^{4+} red–ox couples, respectively. It was established that during prolonged cycling, the electrode potentials of the two plateaus are shifted to more positive values indicating more sluggish kinetics. We presumed that slowing down of the kinetics of these electrodes upon cycling may be the result of the possible formation of surface films on the lithiated oxide electrodes, which leads to an increase of their impedance during cycling [14]. In Figs. 2 and 3, we present impedance spectra of these electrodes as a function of several input parameters such as temperature, cycling and storage duration at a fully intercalated state (E = 3.50 V) and at a partially deintercalated state (E = 4.70 V). The impedance spectra (Nyquist plots) of $LiMO_2$ or $LiM_1M_2O_4$ electrodes (M, M_1, M_2 = Mn, Ni, Co, etc.) are usually described by four major features: high frequency and medium frequency flat semicircles, which can be attributed to surface films and interfacial charge-transfer, respectively (coupled with film

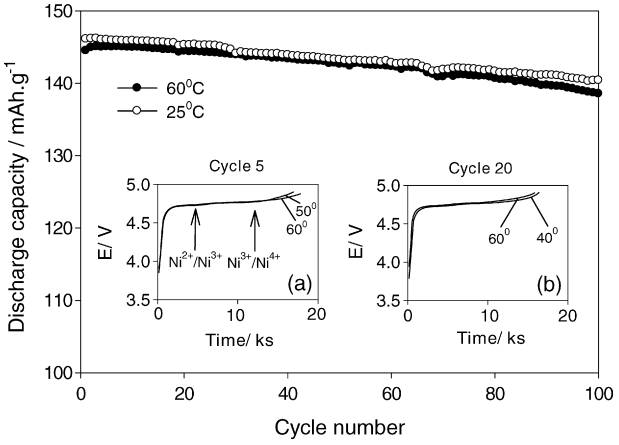

Fig. 1. Discharge capacity of $LiNi_{0.5}Mn_{1.5}O_4$ electrodes measured at 25 and 60 °C as a function of cycle number. Constant current/constant voltage mode (C/5 rate and then potentiostatic step at $E = 4.9$ V, 5 h). Coin-type cells, DMC–EC (2:1)/1.5 M $LiPF_6$ solution. *Insets*: Chronopotentiograms recorded from $LiNi_{0.5}Mn_{1.5}O_4$ electrodes during the 5th cycle at 50 and 60 °C (a) and during the 20th cycle at 40 and 60 °C (b). Constant current mode, C/5 rate. Potential plateaus corresponding to the Ni^{2+}/Ni^{3+} and Ni^{2+}/Ni^{3+} red–ox couples are indicated.

and/or interfacial capacitances), a low frequency "Warburg"-type element that reflects the solid state diffusion of Li-ions, and finally, at the very low frequencies, the Z' versus Z'' plot becomes a steep, nearly vertical line, which reflects the capacitive behavior of the electrode (Li-ion insertion and corresponding charge-transfer). In many cases, the separation among the above major processes and time constants is not clear, and hence, the high-to-medium frequency spectra may appear as a single flat semicircle, which reflects both Li-ion migration through surface films and interfacial charge-transfer [14].

At temperatures of 40 and 50 °C, the impedance of electrodes measured at $E = 3.50$ V changes only slightly with storage compared to electrodes before storage (that underwent a pretreatment of 20 charge/discharge cycles at 100% DOD). At 60 °C, cycling led to an increase in the electrode's impedance, mostly at a high-to-medium frequency (Fig. 3c), which can be related to changes in the electrode surface chemistry.

When studying the electrochemical behavior of $LiNi_{0.5}Mn_{1.5}O_4$ electrodes at different temperatures, it is important to explore how changes in temperature during cycling or storage affect their impedance. In Fig. 4, we compare the impedance responses of $LiNi_{0.5}Mn_{1.5}O_4$ electrodes obtained in two experiments, in which electrodes were treated first at one temperature, measured, after which the temperature was changed, followed by further measurements. In one test, the initial temperature was first changed from 60 to 30 °C and then was returned back to 60 °C (Fig. 4a). A remarkable feature of this experiment is that both resistances R_{sf} and R_{ct} (related mostly to Li-ion migration through surface films and to charge-transfer, reflected by the high and medium frequency semicircles in Fig. 4, respectively) increase at the intermediate temperature of 30 °C (a typical response of an activation-controlled process), and then decrease and become almost unchanged (compared to those measured at the initial temperature) after returning the electrode back to 60 °C. The situation is quite different if the initial temperature was 30 °C, and was then changed to 60 °C, finally being returned to the initial value (Fig. 4b). The resistances to the Li^+ migration through the surface films and that of charge-transfer only changed slightly from $T = 30$ to 60 °C, but then increased substantially after changing the temperature back to $T = 30$ °C. From these results, we conclude that when the initial electrode's surface chemistry is developed at the high temperature (60 °C) it is nearly invariant at a lower temperature as well and, thereby the impedance remains steady. This suggestion is confirmed by the results obtained in separate experiments with pairs

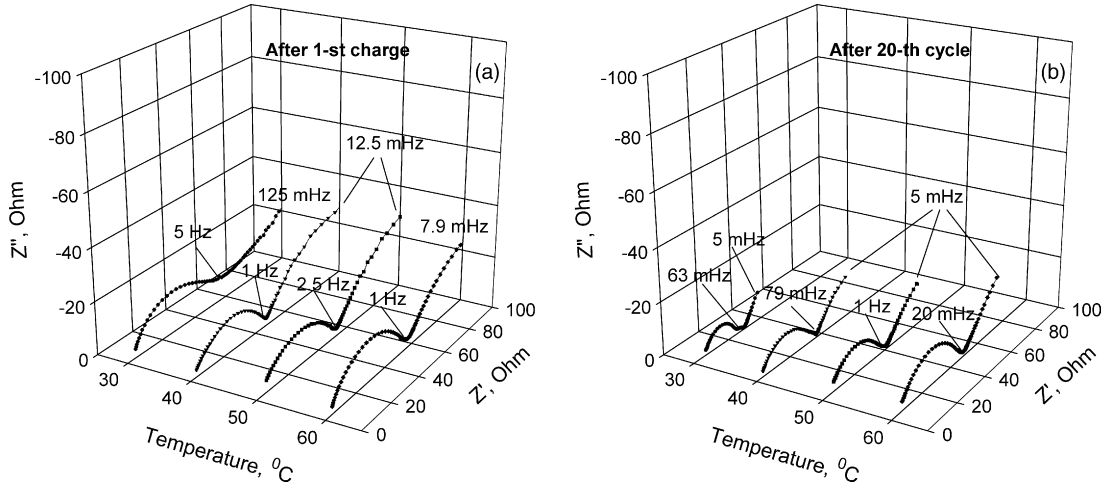

Fig. 2. Impedance spectra (Nyquist plots) obtained at $E = 4.70$ V from $LiNi_{0.5}Mn_{1.5}O_4$ electrodes at various temperatures after the 1st charge to $E = 4.9$ V (a) and after the 20th galvanostatic cycle (b). Constant current mode, C/5 rate. Three-electrode coin-type cells, DMC–EC (2:1)/1.5 M $LiPF_6$ solution.

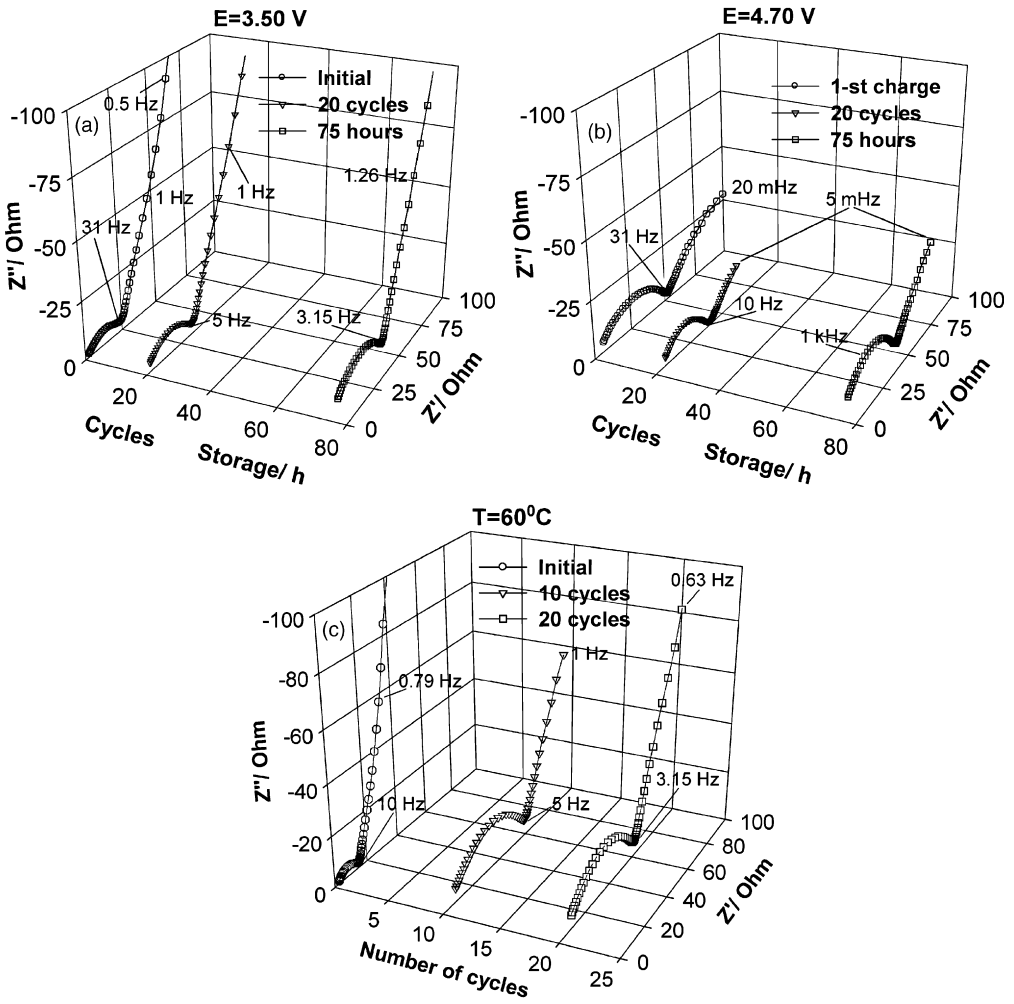

Fig. 3. Impedance spectra (Nyquist plots) measured at 50 °C from $LiNi_{0.5}Mn_{1.5}O_4$ electrodes in a fully intercalated state (a, $E = 3.50$ V) and in a partially deintercalated state (b, $E = 4.70$ V) as a function of cycling and storage time, and at 60 °C, $E = 3.50$ V (c) as a function of cycle number. Constant current mode, C/5 rate. Three-electrode coin-type cells, DMC–EC (2:1)/1.5 M $LiPF_6$ solution.

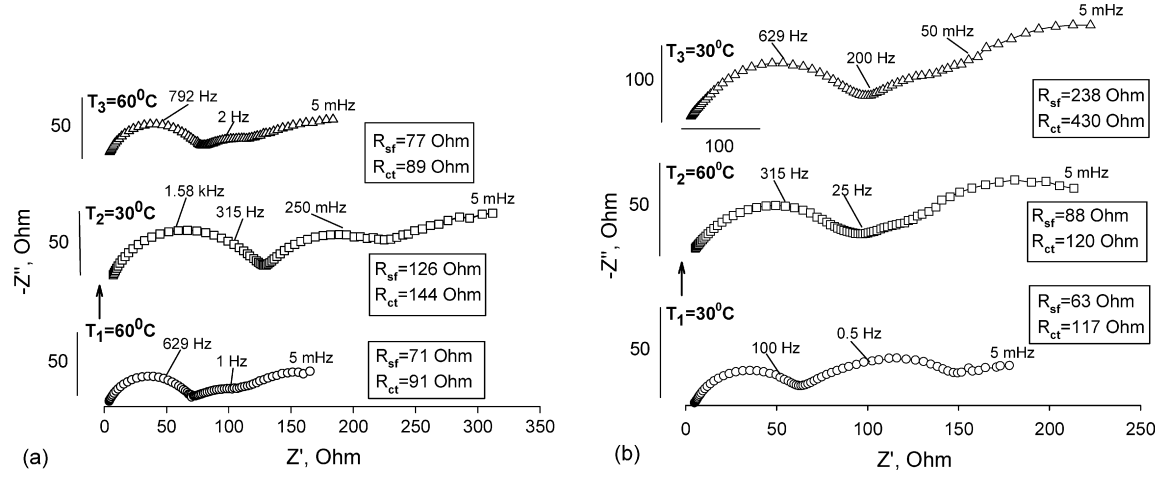

Fig. 4. A comparison of two families of impedance spectra of $LiNi_{0.5}Mn_{1.5}O_4$ electrodes recorded in a partially deintercalated state ($E = 4.70$ V) after charging the electrodes to $E = 4.90$ V. The electrodes were measured initially at 60 or 30 °C, and then the temperature was changed to 30 or 60 °C, followed by impedance measurements. Finally, the temperature was returned to its initial value and the impedance was measured again. (a) The initial electrode's and the measurements temperature was 60 °C and (b) the initial electrode's and the measurements temperature was 30 °C. Arrows show the direction of changes in the electrodes' temperature. Three-electrode coin-type cells, DMC–EC (2:1)/1.5 M $LiPF_6$ solution. Resistances related to Li migration through the electrodes' surface films (R_{sf}) and to the charge-transfer (R_{ct}) calculated from the impedance spectra are presented.

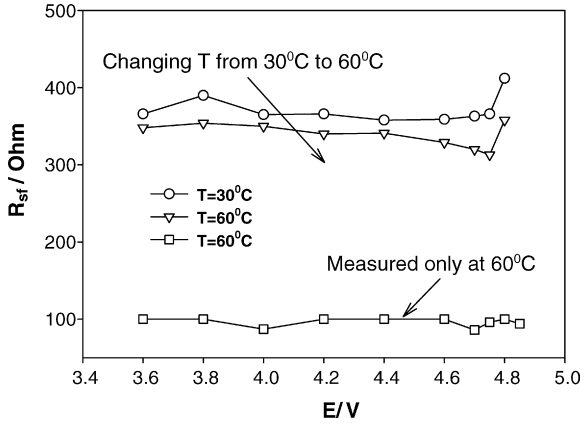

Fig. 5. Dependence of the surface film resistance on the electrodes' potential (Li deintercalation). $LiNi_{0.5}Mn_{1.5}O_4$ electrodes were stabilized by several voltammetric cycles in the 3.50–4.85 V range and impedance was measured first at 30 °C and then at 60 °C, or only at 60 °C, as indicated. Three-electrode coin-type cells, DMC–EC (2:1)/1.5 M $LiPF_6$ solution.

of identical $LiNi_{0.5}Mn_{1.5}O_4$ electrodes. For one electrode, the impedance was measured in a deintercalated state first at 30 °C and then at 60 °C. The second electrode was treated and measured at 60 °C (Fig. 5).

By analyzing the impact of cycling and storage of $LiNi_{0.5}Mn_{1.5}O_4$ electrodes in a wide temperature range (30–70 °C) on their structural characteristics, we came to the following conclusions: only cycling and storage at elevated temperatures (60 °C) causes some changes, such as local Mn and Ni dissolution, and the formation of a new phase of λ-MnO_2 (see the Raman spectrum; Fig. 6e). From the XPS studies of these electrodes (spectra of Ni2p, Ni3p, Mn2p, Fs1, O1s, C1s and Li1s), it is clear that the electrodes' surface becomes rich in LiF, C–F and P–F_x species. We have found that the storage of $LiNi_{0.5}Mn_{1.5}O_4$ electrodes at 60 °C in DMC–EC (2:1)/1.5 M $LiPF_6$ solutions led to both manganese and nickel dissolution [16]. In regard to nickel dissolution, the electrodes' stoichiometry did not change upon storage at 30 and 60 °C for 15 and 7 days, respectively. It was also established that storage at 30 °C and short-time storage at 60 °C in DMC–EC (2:1)/1.5 M $LiPF_6$ solutions (under argon atmosphere) did not result in Mn and Ni dissolution from the electrodes. On the other hand, prolonged storage at 60 °C may lead to pronounced metal dissolution, and hence may cause significant changes in the electrodes' structure and composition. Mn and Ni losses during storage at 60 °C (for 45 days) were 1.3% and up to 50%, respectively. While storage at 30 °C led to minor changes in the Raman spectra of these electrodes, storage at 60 °C resulted in the following major changes, which correlate well with the element analysis related to the Mn and Ni dissolution as presented in Fig. 6: (i) the peak at 407 cm^{-1} corresponding to nickel–oxygen stretching mode [17] almost disappeared and (ii) the intensity of the peak at 500 cm^{-1} (Ni–O bond) decreased significantly in the case of the stored electrode. In addition, a new peak at 575–580 cm^{-1} emerges, which can be attributed to the formation of λ-MnO_2 on the surface of the stored electrode. The results obtained are consistent with the data reported by McLarnon and co-workers in reference [18] where these authors have shown the conversion of a $LiMn_2O_4$ electrode to λ-MnO_2 upon storage at 70 °C in an EC–DMC/$LiPF_6$ solution. It should be noted that a detailed spectroscopic study of the stored $LiNi_{0.5}Mn_{1.5}O_4$ electrode has shown that Raman spectra collected from some other locations on this electrode exhibited a decrease in the intensity of the 407 cm^{-1} peak (indication of partial Ni dissolution), and did not show a new peak of λ-MnO_2. Hence, we conclude that metals (Mn and Ni) dissolve locally from the $LiNi_{0.5}Mn_{1.5}O_4$ active mass by the following mechanism due to an exchange with protons (HF), which may also involve a chemical deintercalation of lithium ions:

$$4LiNi_{0.5}Mn_{1.5}O_4 + 8H^+ \rightarrow 2\lambda\text{-}MnO_2 + Mn^{2+} + Ni^{2+} + 4Li^+ + 4H_2O + 2Ni_{0.5}Mn_{1.5}O_4.$$

The formation of surface λ-MnO_2 (and/or other manganese oxides) was revealed also by a comparative X-ray diffraction study of pristine $LiNi_{0.5}Mn_{1.5}O_4$ electrodes and electrodes after storage. Some additional reflection peaks at 2θ 17.0°, 20.5°, 26.0°, 30.0° and 41.0° in the XRD pattern of the stored electrodes (Fig. 7) may relate to Mn-oxides and to lithium pentafluoromanganate Li_2MnF_5.

3.2. MCMB electrodes

Mesocarbon microbeads are round graphitic particles, which are widely used as an anode material in Li-ion batteries. These spherical particles give a close-packed arrangement in the composite electrodes, resulting in an active mass with high density and very good contact of all the particles with the solution species.

In this work, we focused on studies of cycling/storage behavior and surface reactions of MCMB electrodes at an elevated temperature of 60 °C using SSCV, EIS, SEM and Raman-spectroscopy (the latter tool did not provide significant information for this part of the study). The high temperature and long storage may result in substantial changes in the electrodes' performances (definitely practical conditions for Li-ion batteries).

Two identical sets of MCMB electrodes were chosen for tests in the present study: electrodes of set 1 were cycled by CV in coin-type cells (at a relatively fast scan rate of 2 mV s^{-1} and then at slow rates) at 60 °C in a DMC–EC (2:1)/1.5 M $LiPF_6$ solution, followed by impedance measurements during Li intercalation (from 300 to 10 mV). The electrodes were then stored at 60 °C for 30, 60 and 180 days, at the charged state (OCV around 50–85 mV versus Li/Li^+). After each of these periods of storage, slow scan rate CV (5 μV s^{-1}) and impedance were measured from these electrodes at 60 °C.

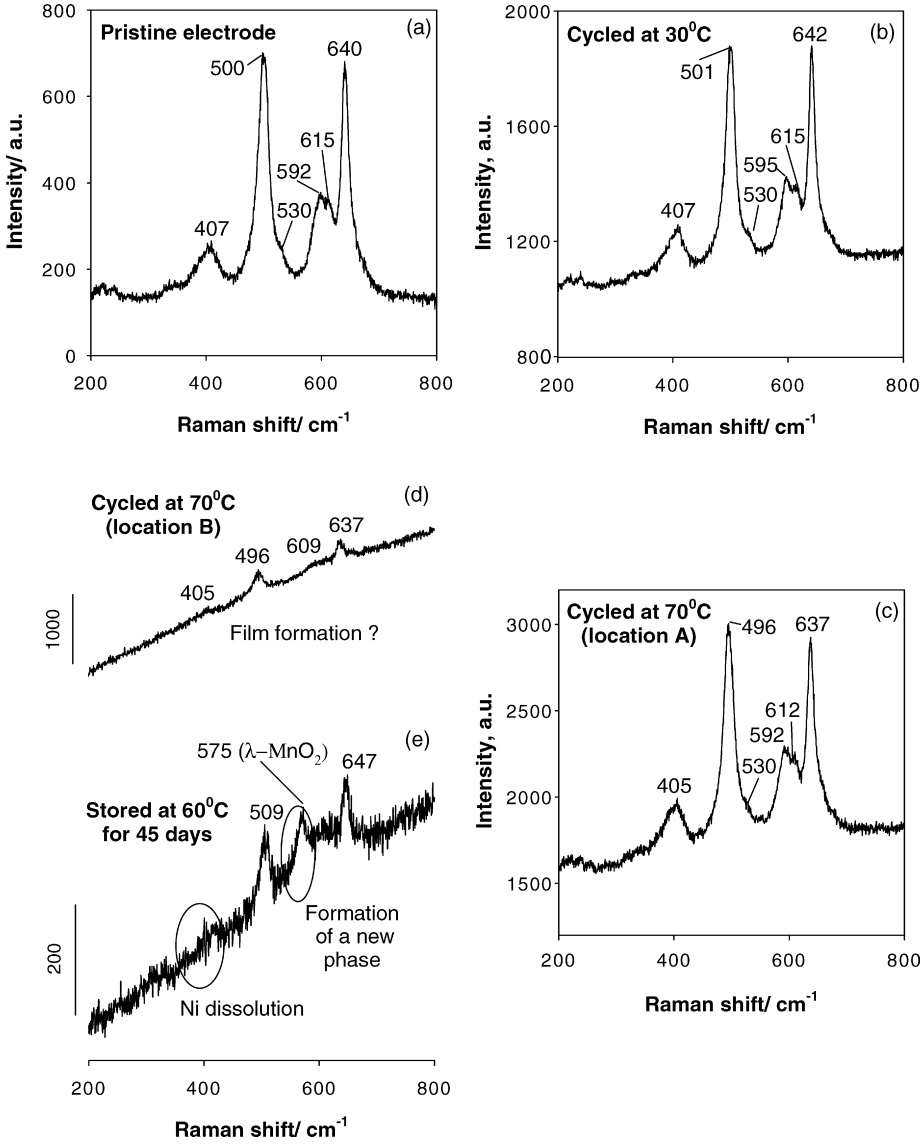

Fig. 6. Ex situ Raman spectra of a pristine $LiNi_{0.5}Mn_{1.5}O_4$ electrode (a) and of electrodes after several voltammetric cycles at 30 °C (b) and at 70 °C. (c and d) Present spectra recorded from different locations on the electrode's surface. Cycling tests were performed in flooded cells with electrodes comprising only the active $LiNi_{0.5}Mn_{1.5}O_4$ particles embedded in Al foils, free of carbon black and PVdF binder. After cycling, the electrodes were kept potentiostatically at $E = 3.50$ V for 20 h. (e) The Raman spectrum of a composite $LiNi_{0.5}Mn_{1.5}O_4$ electrode stored in a DMC–EC (2:1)/1.5 M $LiPF_6$ solution at 60 °C for 45 days.

The experiments with the electrodes of set 2 were quite similar to those of the other set of electrodes. The difference was that the electrodes of set 2 were stored at 60 °C (15 days, at OCV) in the above solution prior to their electrochemical cycling. Although the graphite/carbon electrodes are not supposed to be reactive with EC–DMC/$LiPF_6$ solutions at OCV before lithiation, some surface reactions may occur at elevated temperatures (e.g. surface oxidation of carbon).

The results of slow scan rate voltammetric cycling of both types of electrodes (1 and 2) are shown in Fig. 8. Similar to graphite electrodes, MCMB demonstrates clear reversible behavior, as is well documented in the literature and which reflects phase transitions between Li intercalation stages (e.g., the two major sets of peaks at 0.101 and 0.067 V in Fig. 8 relate to phase transitions between stages 3 and 2 (LiC_{16} is formed) and between stages 2 and 1 that forms LiC_8, respectively [19,20]. Both types of electrodes (1 and 2) show similar currents during their first slow scan rate cycling to 0 V and back to high potentials, and also show the same voltammetric peaks. The difference is that these peaks are broader for type 2 electrodes, indicating some kinetic limitations. A remarkable finding is that electrodes of type 2 demonstrate a larger initial discharge and charge capacities compared to type 1 electrodes (Fig. 9). This is surprising, especially when taking into account the results of the morphological and structural studies of both electrodes. From the insets in Fig. 8, which show SEM images of electrodes 1 and 2, it is clearly seen that electrode 2 underwent dramatic morphological changes due to prolonged storage at 60 °C (OCV conditions), prior to its intercalation with lithium

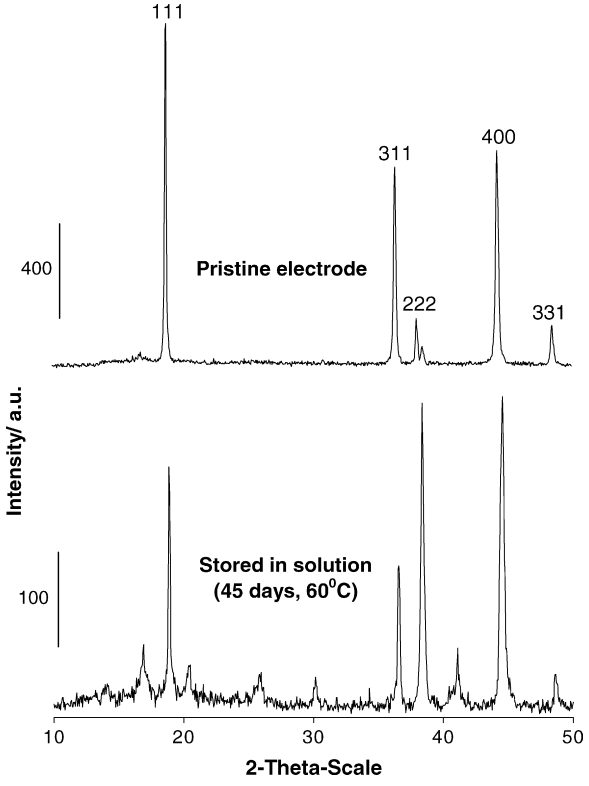

Fig. 7. XRD patterns of a pristine $LiNi_{0.5}Mn_{1.5}O_4$ electrode and of an electrode stored in a DMC–EC (2:1)/1.5 M $LiPF_6$ solution at 60 °C for 45 days.

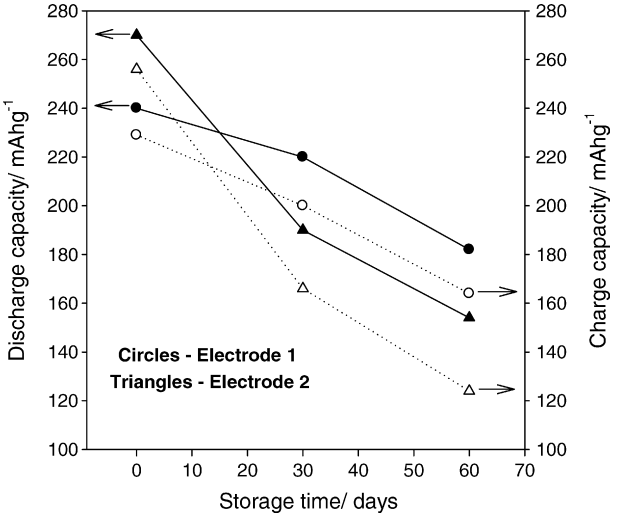

Fig. 9. Charge and discharge capacities of the MCMB electrodes (1 and 2) calculated from the CVs (Fig. 8) as a function of storage time.

and cycling. Its micrograph (Fig. 8b) shows ball-like particles of a super P conductive additive (50–500 nm in size) on the surface of the MCMB particles (beads of 10 μm). We should note that no morphological changes have occurred with MCMB particles after their storage at 60 °C for 15 days (SEM images are not shown here). It is presumed that electrode storage in the solution at OCV, leads to an exposure of super P carbon nanoparticles. This could occur due to the swelling of the binder at the elevated temperature, during prolonged storage [21]. This phenomenon however does not influence pronouncedly the electrochemical response of the electrodes (see the CVs in Fig. 8). By comparing the XRD patterns of electrodes 1 and 2 (Fig. 10) we conclude that the additional reflection at $2\theta = 38.5^\circ$ in the pattern of electrode 2 may reflect the formation of lithium fluoride on the electrodes' surface due to the thermal decomposition of $LiPF_6$

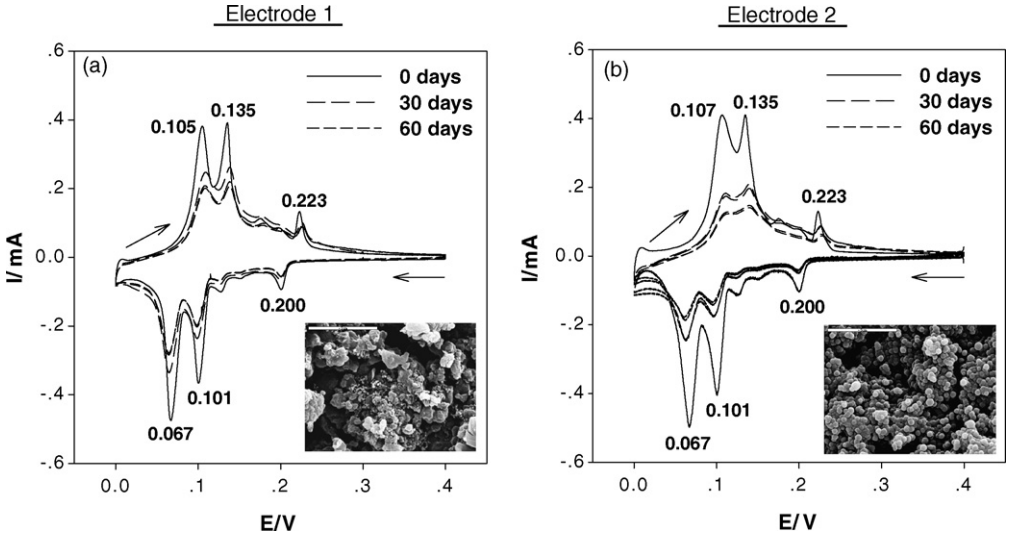

Fig. 8. Cyclic voltammograms (CVs) of two identical composite MCMB electrodes (1 and 2) measured at a scan rate of 5 μV s^{-1} at 60 °C, at the initial state (0 days) and after storage of the MCMB/Li cells at 60 °C for 30 and 60 days in a charged state (OCV potential around 50–85 mV vs. Li/Li^+). Electrode 2 was stored at OCV around 3 V vs. Li/Li^+ in a DMC–EC (2:1)/1.5 M $LiPF_6$ solution (60 °C, 15 days) prior to cycling. The numbers near the CVs indicate the potentials of the voltammetric peaks. Three-electrode coin-type cells, DMC–EC (2:1)/1.5 M $LiPF_6$ solution. *Insets*: SEM micrographs of a pristine MCMB electrode 1 (a) and of an electrode 2 stored in the above solution at 60 °C for 15 days (b). Solution volume was 10 mL, geometric area of the electrode was 1.54 cm^2. Scales of 5 μm appear in the micrographs.

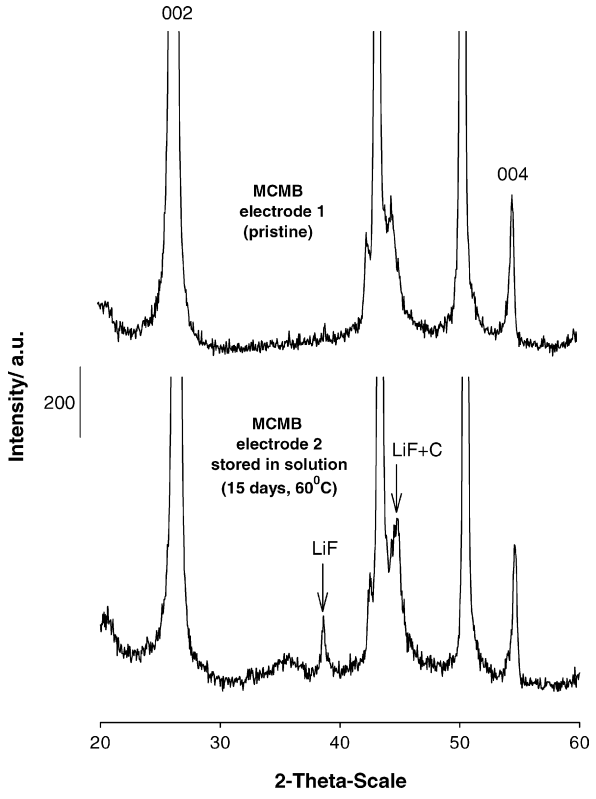

Fig. 10. XRD patterns of a pristine MCMB electrode (type 1) and of an electrode type 2 stored in a DMC–EC (2:1)/1.5 M $LiPF_6$ solution at 60 °C for 15 days, at OCV conditions.

($LiPF_6 \rightarrow LiF + PF_5$) that may be catalyzed by the carbon (super P) nanoparticles.

In Figs. 11 and 12, we compare the impedance spectra measured from MCMB electrodes 1 and 2 at various potentials during Li intercalation. The aim was to study to what extent storage of the MCMB electrodes for 15 days at 60 °C in a solution, prior to cycling and prolonged storage of MCMB/Li cells at 60 °C, influences the impedance characteristics. Note that the electrodes were stored at 60 °C for 30, 60 and 180 days at the charged state, and after each of these periods of storage, slow scan rate CV (5 μV s^{-1}) and impedance were measured from these electrodes at 60 °C. As seen in Figs. 11 and 12, the electrodes' aging at 60 °C changes their impedance spectra pronouncedly. The electrodes' impedance increases by an order of magnitude due to storage. We attribute the high-to-medium frequency features of the spectra, which appear as flat semicircles, to the contribution of the surface films, which cover the active mass [15 and references therein], and to the electrodes' impedance (e.g. resistance to Li-ions migration coupled with film and interfacial capacitive elements). The increase in the electrodes' impedance due to aging is expected and has been well discussed in the literature [22]. It is very significant that the high-to-medium (semicircle type) features in the impedance spectra of both types of electrodes are nearly potential invariant, as demonstrated in Fig. 13. Comparing Figs. 11 and 12 shows that the high-to-medium frequency impedance of the type 2 electrodes is higher compared to that

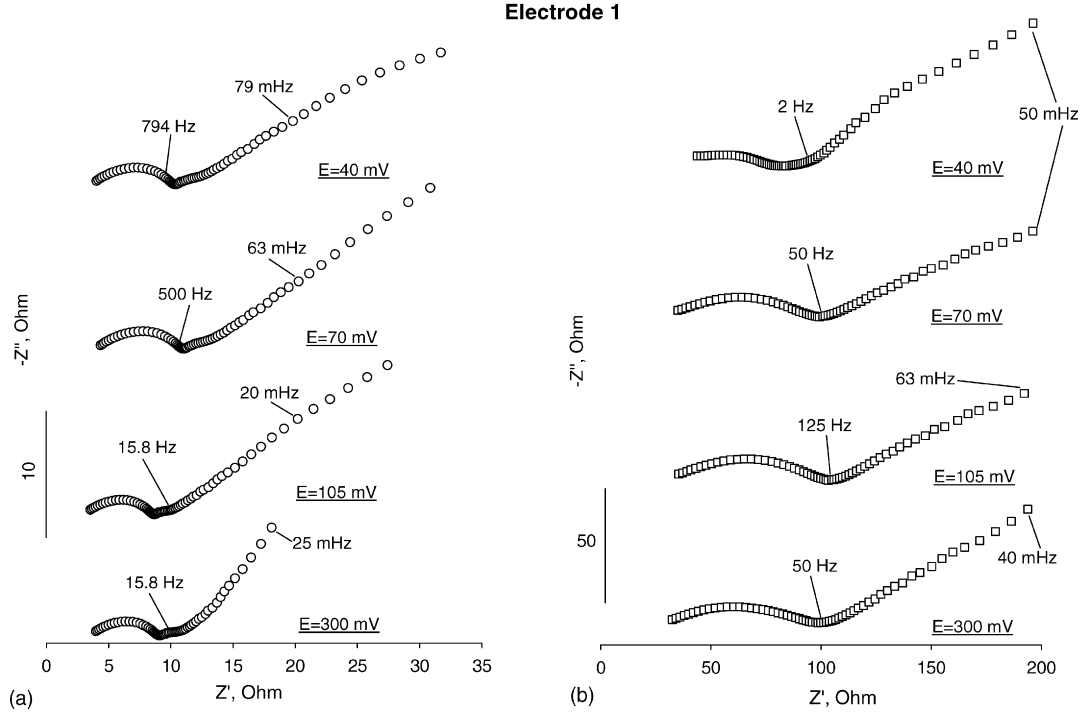

Fig. 11. Impedance spectra obtained at 60 °C from the MCMB electrode type 1 (see text) at various potentials of Li^+ intercalation, as indicated: (a) the electrode's initial state (0 days) and (b) after storage of the MCMB/Li cell at 60 °C for 180 days. The electrode was stored at 60 °C for 30, 60 and 180 days at the charged state in the MCMB/Li cells and after each of these periods of storage, slow scan rate CV (5 μV s^{-1}) and impedance were measured at 60 °C. Three-electrode coin-type cells, DMC–EC (2:1)/1.5 M $LiPF_6$ solution.

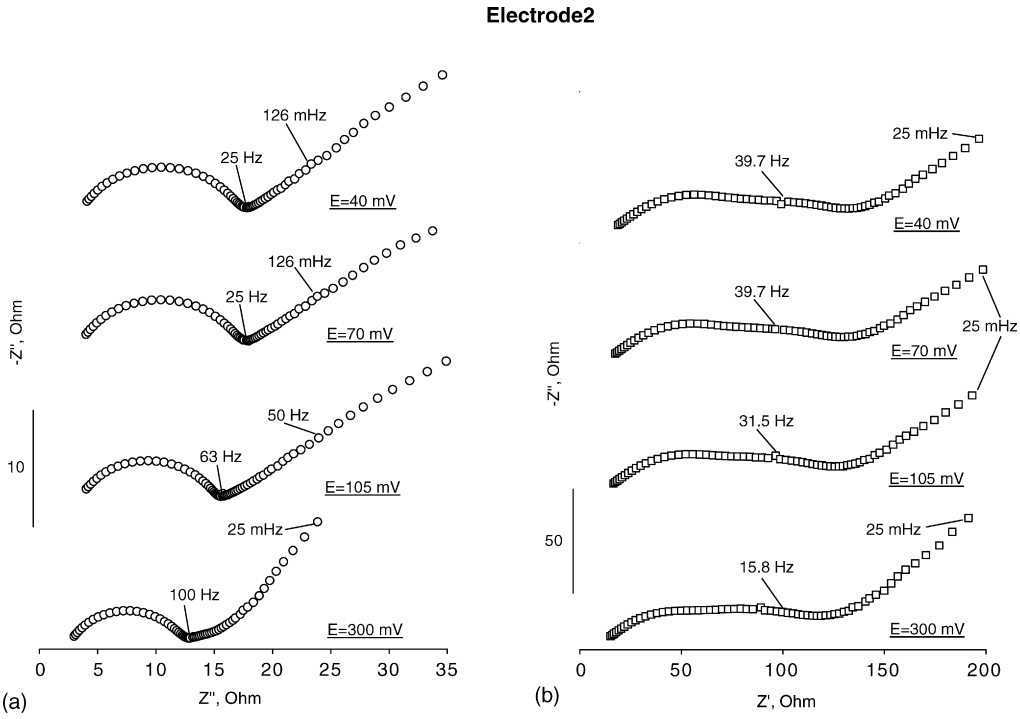

Fig. 12. Same as Fig. 11. MCMB electrode 2, which was stored at OCV at 60 °C for 15 days, before cycling.

of type 1 electrodes. The ageing of type electrodes 2 leads to a pronounced broadening of their high-to-medium frequency impedance. We attribute this broadening and the relatively higher impedance of type 2 electrodes (storage at 60 °C at OCV before lithiation) to the enhanced formation of LiF due to the decomposition of $LiPF_6$, and to a lesser interparticle contact due to some swelling of the binder. $LiPF_6$ thermal decomposition forms PF_5 that can be further reduced to LiF and Li_xPF_y species. LiF forms highly resistive films on Li and Li–C electrodes [15 and references therein]. Bad interparticle contact in the composite electrodes should lead to a non-uniform behavior of the active mass and hence to their electrochemical response via a dispersion of time constants. This is indeed well expressed by the broad impedance of the electrodes that were aged before their lithiation. Hence, one can conclude that it is preferable not to let these MCMB electrodes age in solutions at OCV, but rather proceed with fast lithiation soon after the composition of the cells (after the active mass is well impregnated by the electrolyte solution). A first lithiation forms the surface films, which contribute to the mechanical stability of the composite electrodes. Therefore, aging composite MCMB electrodes at elevated temperatures after the surface films are formed and stable (i.e. after their first lithiation), may be less problematic and detrimental to their integrity and cycling stability, than aging the pristine electrodes in solutions at OCV.

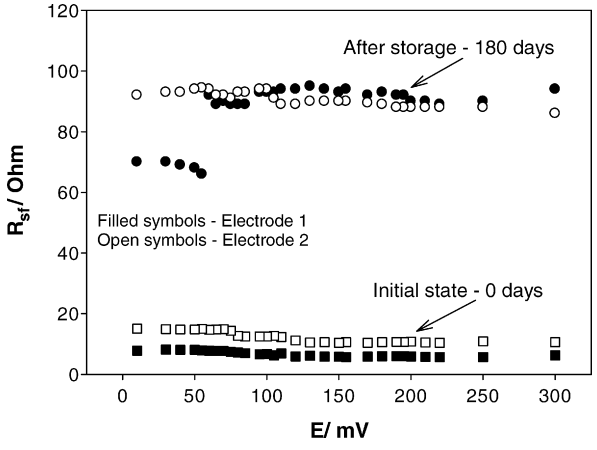

Fig. 13. Dependence of the resistance attributed to the surface films R_{sf}, measured from the high-to-medium frequency domain of the impedance spectra (the semicircle like part of the spectra) of the MCMB electrodes 1 and 2 at their initial state (0 days) and after storage in the MCMB/Li cells at the charged (lithiated) state at 60 °C for 180 days.

4. Conclusions

1. It was concluded that more sluggish electrochemical kinetics during the prolonged cycling of $LiNi_{0.5}Mn_{1.5}O_4$ electrodes at elevated temperatures (40–60 °C) may be related mostly to the formation of surface films on these electrodes, which leads to an increase in their impedance, and not to a pronounced degradation of the active mass. The surface chemistry developed is important for the cycling performance and storage behavior of the elec-

trodes. The XPS measurements prove the precipitation of LiF, C–F and P–F_x species as well as organic compounds (probably, polyethers) on the electrodes.

2. We have found that the surface chemistry of $LiNi_{0.5}Mn_{1.5}O_4$ electrodes depends strongly on the temperature. This is clear from impedance measurements performed first at low temperature (30 °C), then at high temperature (60 °C), and finally at 30 °C. It was demonstrated that when the initial electrode's surface chemistry is developed at the high temperature (60 °C), it is nearly invariant at a lower temperature as well, and thereby, the impedance remains steady.
3. From the micro-Raman measurements, we have shown that the $LiNi_{0.5}Mn_{1.5}O_4$ active mass is stable in its structure upon prolonged cycling/storage at 30 °C. At high temperatures (60–70 °C), there are changes in the surface/bulk of the active mass correlated with dissolution of Mn and Ni and the formation of λ-MnO_2. However, these changes are not uniform, but rather localized, occurring in selected domains of the active mass.
4. The storage of MCMB electrodes at 60 °C in DMC–EC/$LiPF_6$ solutions at OCV conditions (around 3 V versus Li/Li^+), leads to the formation of lithium fluoride on the electrodes' surface (as established by XRD studies) due to the thermal decomposition of $LiPF_6$. Prolonged ageing of composite MCMB electrodes at elevated temperatures seems to have a minor impact on their cycling behavior after these electrodes have been stabilized by surface films during first lithiation.

References

[1] Y. Ein-Eli, W.F. Howard Jr., S.H. Lu, S. Mukerjee, J. McBreen, J.T. Vaughey, M.M. Thackeray, J. Electrochem. Soc. 145 (1998) 1238.
[2] K.A. Striebel, A. Rougier, C.R. Horne, R.P. Reade, E.J. Cairns, J. Electrochem. Soc. 146 (1999) 4339.
[3] T. Ohzuku, S. Takeda, M. Iwanaga, J. Power Sources 81–82 (1999) 90.
[4] H. Kawai, M. Nagata, H. Kageyama, H. Tukamoto, A.R. West, Electrochim. Acta 45 (1999) 315.
[5] H.J. Bang, V.S. Donepudi, J. Prakash, Electrochim. Acta 48 (2002) 443.
[6] Y.-K. Sun, K.-J. Hong, J. Prakash, K. Amine, Electrochem. Commun. 4 (2002) 344.
[7] R. Alcantara, M. Jaraba, P. Lavela, J.L. Tirado, Ph. Biensan, A. de Guibert, C. Jordy, J.P. Peres, Chem. Mater. 15 (2003) 2376.
[8] Y. Shin, A. Manthiram, Electrochim. Acta 48 (2003) 3583.
[9] R. Alcantara, M. Jaraba, P. Lavela, J.M. Lloris, C. Perez Vicente, J.L. Tirado, J. Electrochem. Soc. 152 (2005) A13.
[10] Y. Ein-Eli, W. Wen, S. Mukerjee, Electrochem. Solid State Lett. 8 (2005) A141.
[11] K. Tatsumi, N. Iwashita, H. Sakaebe, H. Shioyama, S. Higuchi, A. Mabuchi, H. Fujimoto, J. Electrochem. Soc. 142 (1995) 716.
[12] M. Inaba, H. Yashida, Z. Ogumi, J. Electrochem. Soc. 143 (1996) 2572.
[13] I.R. Alcantara, F.J.F. Madrigal, P. Lavela, J.L. Tirado, J.M.J. Mateos, C.G. de Salazar, R. Stoyanova, E. Zhecheva, Carbon 38 (2000) 1031.
[14] B. Markovsky, Y. Talyossef, G. Salitra, D. Aurbach, H.-J. Kim, S. Choi, Electrochem. Commun. 6 (2004) 821;
D. Aurbach, M.D. Levi, E. Levi, H. Teller, B. Markovsky, G. Salitra, H. Heider, L. Heider, J. Electrochem. Soc. 145 (1998) 3024.
[15] D. Aurbach, B. Markovsky, M.D. Levi, E. Levi, A. Schechter, M. Moshkovich, Y. Cohen, J. Power Sources 81–82 (1999) 95.
[16] Y. Talyossef, B. Markovsky, G. Salitra, D. Aurbach, H.-J. Kim, S. Choi, 12th IMLB, J. Power Sources 146 (2006) 664–669.
[17] K. Dokko, M. Mohamedi, N. Anzue, T. Itoh, I. Uchida, J. Mater. Chem. 12 (2002) 3688.
[18] Y. Matsuo, R. Kostecki, F. McLarnon, J. Electrochem. Soc. 148 (2001) A687.
[19] A. Mabuchi, H. Fujimoto, K. Takumitsu, T. Kasuh, J. Electrochem. Soc. 142 (1995) 3049.
[20] T. Kasuh, A. Mabuchi, K. Takumitsu, H. Fujimoto, J. Power Sources 68 (1997) 99.
[21] M. Yoo, C.W. Frank, S. Mori, S. Yamaguchi, Chem. Mater. 16 (2004) 1945.
[22] B. Markovsky, A. Rodkin, Y.S. Cohen, O. Palchik, E. Levi, D. Aurbach, H.-J. Kim, M. Schmidt, J. Power Sources 119–121 (2003) 504.